Buckling and Collapse of Embedded Carbon Nanotubes

O. Lourie,[1] D. M. Cox,[1,2] and H. D. Wagner[1,*]

[1]*Department of Materials & Interfaces, The Weizmann Institute of Science, Rehovot 76100, Israel*

[2]*Exxon Research and Engineering, Route 22 East, Annandale, New Jersey 08801*

(Received 20 November 1997)

Experimental observations of various deformation and fracture modes under compression of single multiwalled carbon nanotubes, obtained as a result of embedment within a polymeric film, are reported. Based on a combination of experimental measurements and the theory of elastic stability, the compressive strengths of thin- and thick-walled nanotubes are found to be about 2 orders of magnitude higher than the compressive strength of any known fiber. [S0031-9007(98)06940-3]

PACS numbers: 61.48.+c, 62.20.–x

Recent experimental and theoretical results [1–9] suggest that carbon nanotubes hold great promise as a possible reinforcing phase in composite materials of a new kind. Such developments still present, however, enormous practical challenges, especially when probing the properties of individual nanotubes [3,10–12]. The mechanical stiffness and strength of carbon nanotubes are expected to be very high [2,4,8]. Also, breaks in nanotubes, either in tension or compression, were rarely observed following specimen cutting [9,12], which was taken to imply that nanotubes have very high strength [9]. It is remarkably difficult to directly measure the mechanical properties of single nanotubes. The stiffness of carbon nanotubes was recently measured by a thermal vibration technique [3] and Young's modulus was reported to be in the 1–5 TPa range. (The modulus of diamond, one of the stiffest known materials, is 1.2 TPa [13].) Here we report deformation modes resulting from the embedment of the tubes in a polymer matrix, and a first estimation of the strength of carbon nanotubes under compressive stresses.

Multiwall carbon nanotubes, prepared by a carbon-arc discharge method, were sonicated in ethanol and subsequently dried and dispersed on a glass surface. An epoxy resin (Araldite LY564, Ciba-Geigy) was used as embedding medium. The liquid polymer mixture was carefully spread onto the dried nanotube-containing graphite powder using a blade. The mixture was polymerized in a closed mold for five days at room temperature. This procedure produced 200–300 μm thick rigid amorphous polymer composite films. The polymer films were microtomed into thin (70–100 nm) slices in a direction parallel to the film surface, using a diamond knife and a Reichert-Jung ultracut microtome (at room temperature). The slices were then examined by transmission electron microscopy (TEM) using a Philips EM400T at 100 kV. The TEM work was made particularly difficult by the presence (and thickness) of the polymer, which strongly reduces the image contrast. Thus we studied only those tubes that were close to or at the polymer surface. Extensive observations revealed that nanotubes collapsed under a compressive stress through a variety of deformation modes, depending mostly on the tube morphology and geometry. The compressive stress arises from polymerization shrinkage as well as from thermal effects associated with the electron beam in the TEM cell. The latter is significant but difficult to estimate, and for the room temperature curing epoxy used here, the measured linear contraction due to polymerization only was $(5.4 \pm 1.4)\%$.

The behavior under stress of carbon nanotubes was found to strongly depend on the tube geometry and structure. Nanotubes prepared by current methods are inevitably produced with a wide range of geometries, and thus may be thick or thin walled and possess a range of length-to-diameter ratios. The wall thickness h may easily be converted from the number of graphitic layers, based on the average interwall separation of 3.4 Å. We observed that slender nanotubes (for which $L \gg r$, where L and r are the tube length and outer radius, respectively) mostly deform by buckling (Figs. 1 and 2), as an elastica [14], provided that they are thick walled ($h/r > \sim 0.6$). The tubes are forced through the thin surface layer of matrix and bend sideways by a large amount. The stress at which this occurs is given by [15–18]

$$\sigma_{\text{crit}} = E_{\text{NT}}(m\pi r/L)^2 + (2K/\pi)(L/m\pi r)^2, \qquad (1)$$

where E_{NT} denotes the Young's modulus of the nanotubes, the integer m is the number of half waves in which the nanotube subdivides at buckling, and K is the foundation modulus, which reflects the fiber-matrix interaction [16,17]. The latter may be strong ($K_{\max}$) or weak ($K_{\min}$), as follows [17]

$$K_{\max} = \frac{4\pi E_m(1-\nu)/(1+\nu)}{(3-4\nu)K_0(m\pi r/L)}, \qquad (2)$$

$$K_{\min} = \frac{4\pi E_m(1-\nu)/(1+\nu)}{(3-4\nu)K_0(m\pi r/L) + (m\pi r/L)K_1(m\pi r/L)}, \qquad (3)$$

where E_m and ν are the matrix Young's modulus and Poisson ratio, respectively, and K_0 and K_1 are the modified Bessel functions of the second kind. As mentioned above, the integer m is the number of half waves in which

 0031-9007/98/81(8)/1638(4)$15.00

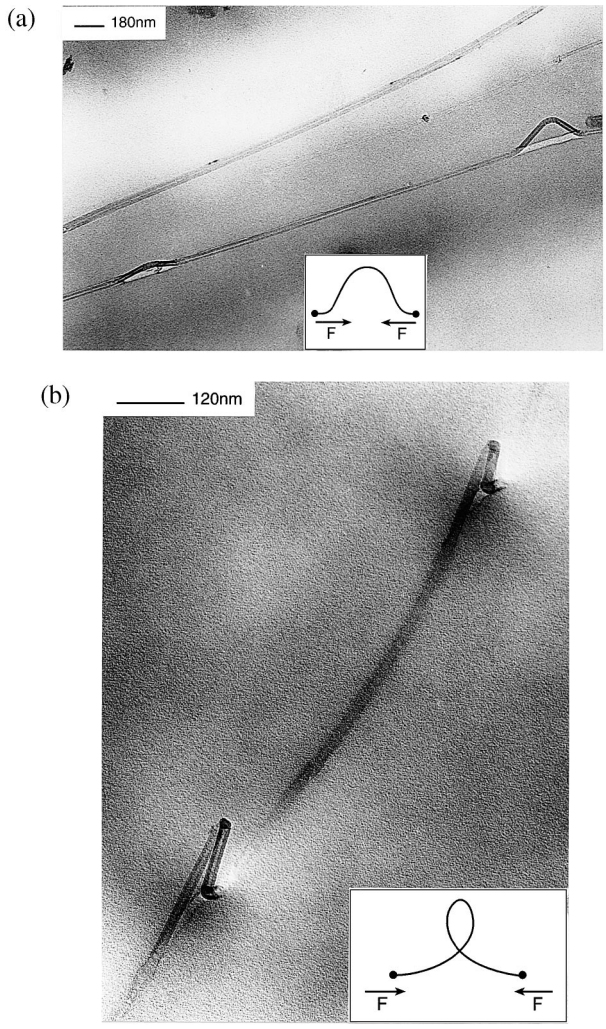

FIG. 1. TEM micrographs of long and slender multiwall carbon nanotubes which, under compression, behave as elastica rods and form bends (a) and loops (b).

the nanotube subdivides at buckling but is effectively used [17] to minimize Eq. (1). The first term on the right hand side in Eq. (1) is the classical Euler formula for buckling assuming that the tube ends are built in, that is, prevented from rotating during buckling [16]. The second term represents the contribution of the matrix [17]. Sideways buckling may result in open or closed loops, and we indeed observed both modes [Figs. 1a and 1b]. The compressed side of the nanotubes may undergo yielding and local inward compressive buckling, as seen in Fig. 2. Our experimental observations are strikingly similar to the theoretical predictions of Yakobson *et al.* [8] and Iijima *et al.* [2], even though these authors considered free tubes (no matrix).

In the top portion of Table I we report buckling data for selected tubes with a fairly uniform geometry ($h/r \approx 0.72$). The variation of the critical buckling stress, calculated by means of Eq. (1) (using the conservative value of 1.2 TPa for the Young's modulus of nanotubes), with

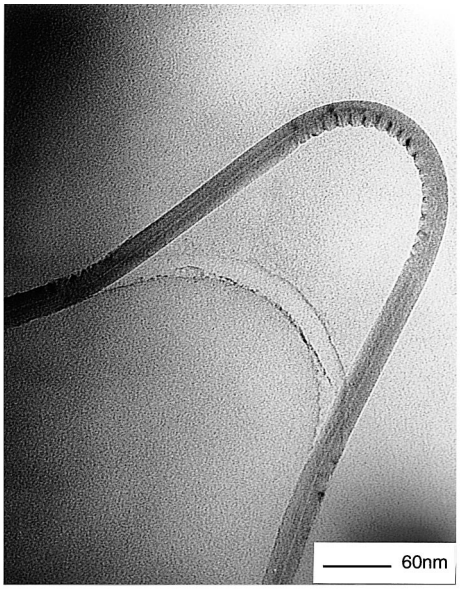

FIG. 2. Under high bending, nanotubes collapse to form kinks on the internal (compression) side of the bend, which fits the predictions of Refs. [2,8].

the measured buckling length is plotted in Fig. 3. As the buckling length L decreases, the stress increases rapidly and from a physical viewpoint, compressive crushing progressively becomes the preferred fracture mode. However, we did not observe this fracture mode, probably because the stress necessary to induce it in thick-walled tubes is very high. The smallest observed buckling length was of the order of $L/r = 10.5$, corresponding to a compressive stress of 135 GPa for a weak interface and 147 GPa for a strong interface. These values may, thus, be viewed as lower bounds for the crushing (or compressive) strength of this group of (thick-walled) nanotubes, as indicated in Fig. 3. As seen, the effect of interfacial adhesion on the buckling stress is relatively minor. Table I and Fig. 3 reveal that, for small values of L/r, the presence of the matrix results in at least a 30% increase of the critical stress (thus, compressed free nanotubes would buckle at lower stresses).

Contrasting with the above, thin-walled tubes were observed to mostly collapse, or possibly fracture, rather than buckle, under compression. Using the theory of thin shells, Yakobson *et al.* [8] predicted that slender single-wall nanotubes would buckle locally into a variety of morphological patterns corresponding to singularities in the strain energy profile. We did not detect such patterns [19], possibly because Yakobson *et al.* [8] considered free rather than embedded nanotubes. Moreover, the thin-walled tubes examined here are not strictly single walled and are not as slender as those considered by Yakobson *et al.* [8]. Instead, we observed that embedded thin-walled tubes fail by compressive collapse or crushing, which manifests itself by the progressive fragmentation of tubes (Fig. 4). Measurements were performed with

TABLE I. Experimental data for the compressive collapse of thick-walled and thin-walled carbon nanotube leading to (a) buckling and (b) collapse (fragmentation), respectively. The buckling stress σ_{crit} was calculated from Eq. (1) using $E_n = 1.2$ TPa, $E_m = 2$ GPa, $\nu_f = 0.25$, and $\nu = 0.35$, for each value of L/r, using the value of m (rounded to the closest integer) that minimizes σ_{crit}.

Outer diameter $2r$ (nm)	h/r	Buckling length L (nm)	L/r	σ_{EULER} $(m = 1)$ (GPa)	m	σ_{crit} (min) (GPa)	σ_{crit} (max) (GPa)
		(a) Buckling					
10.4	0.75	54.8	10.5	107.4	1	135.0	146.5
17.3	0.74	90.9	10.5	107.4	1	135	146.5
7.3	0.81	47	12.9	71.3	1	108.9	123
7.3	0.75	48.9	13.4	66.0	1	105.9	120.6
16.6	0.6	117	14.1	59.6	1	102.8	118.4
17.7	0.75	164.7	18.6	34.2	1	101.2	122.3
10.7	0.66	128.4	24	20.6	2	116.0	129.1
16.5	0.66	223.5	27.1	16.1	2	105.2	120.1

Outer diameter $2r$ (nm)	Relative wall thickness h/r	Mean fragment length $\langle L \rangle$ (nm)
	(b) Collapse	
19.6	0.08	74.4
20	0.08	65
56.2	0.07	90.4
30.8	0.09	81.2
30	0.07	85
30	0.07	76
56.2	0.07	140
20	0.1	60

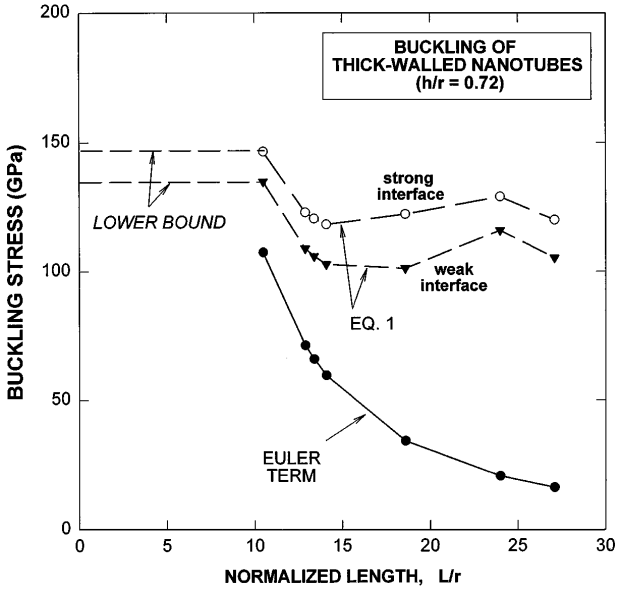

FIG. 3. Strength under compression of thick-walled carbon tubes as a function of measured buckling length, using Eqs. (1)–(3) [17]. Buckling is predominant for long tubes, whereas crushing progressively arises for shorter tubes. The Euler term was calculated using $m = 1$.

thin-walled ($h/r \approx 0.08$) nanotubes for which the failure mode was crushing, or compressive fragmentation, and the data are reported in the lower part of Table I. In this case, approximate lower and upper bounds for the compressive strength can be obtained. Taking twice the measured average fragment length as the smallest conceivable buckling length (thus $2\langle L \rangle = 168$ nm), a stress of 139.8 GPa is calculated using Eq. (1), in the case of a weak interface, using $L/r = 10.3$, $E_n = 1.2$ TPa, and $m = 1$. This may thus be considered as an upper bound for the compressive strength of this group of (thin-walled) nanotubes [20], with a weak interface. The actual length at which buckling rather than crushing is the preferred mode is conceivably larger, and we may take the length of the full tube, typically 1 μm on average, as an upper limit. The corresponding lower bound [from Eq. (1), again in the case of a weak interface] is 99.9 GPa, using $L/r = 60.9$, $E_n = 1.2$ TPa, and $m = 4$. Similar calculations for the case of a strong interface lead to upper and lower bounds of 151 and 116.7 GPa, respectively.

We conclude that the compressive strength of thin- and thick-walled nanotubes is more than 2 orders of magnitude higher than the compressive strength of any known fiber (which lies in the 0.5 GPa range). A lower, but still comparatively high range of nanotube compressive

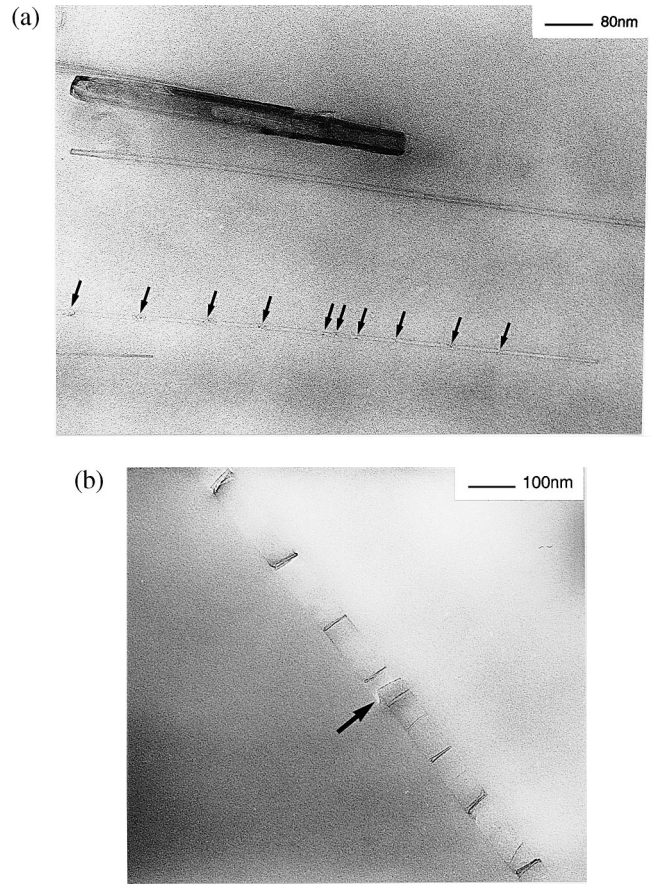

FIG. 4. TEM photographs of compressive crushing patterns similar to those observed in fragmentation tests of single-fiber composite materials: (a) sites of compressive collapse (indicated by arrows) in a small diameter, thin-walled nanotube and (b) in a flattened, large diameter, thin-walled nanotube (note the presence of a fold, indicated by the arrow).

strengths is obtained when a calculation based on the linear contraction $\varepsilon_{\text{curing}}$ arising from polymer curing is performed. Indeed, using $E_n = 1.2$ TPa [3], and Hooke's law $\varepsilon_{\text{curing}} = \sigma_m/E_m = \sigma_n/E_n$, where the subscripts m and n stand for matrix and nanotube, respectively, one obtains a compressive strength of ~60 GPa. Note again that the contraction is probably higher, due to thermal effects in the TEM cell, and that it is also conceivable that the modulus of the nanotubes is larger than 1.2 TPa [3].

For strong fibers used in the composite materials field, the ratio of compressive to tensile strength is (10–30)%: If the same applies to carbon nanotubes, very high tensile strengths are predicted, based on the results presented here.

We are grateful to S. Safran and S. Weiner for fertile discussions and suggestions.

*Author to whom correspondence should be addressed.
Email address: cpwagner@wis.weizmann.ac.il

[1] S. Iijima, Nature (London) **354**, 56 (1991).
[2] S. Iijima, C. Brabec, A. Maiti, and J. Bernholc, J. Chem. Phys. **104**, 2089 (1996).
[3] M. M. J. Treacy, T. W. Ebbesen, and J. M. Gibson, Nature (London) **381**, 678 (1996).
[4] G. Overney, W. Zhong, and D. Tomanek, Z. Phys. D **27**, 93 (1993).
[5] D. H. Robertson, D. W. Brener, and J. W. Mintmire, Phys. Rev. B **45**, 12 592 (1992).
[6] N. Chopra, L. Benedict, V. Crespi, M. Cohen, S. Louie, and A. Zettl, Nature (London) **377**, 135 (1995).
[7] J. M. Molina, S. S. Savinsky, and N. V. Khokhriakov, J. Chem. Phys. **104**, 4652 (1996).
[8] B. I. Yakobson, C. J. Brabec, and J. Bernholc, Phys. Rev. Lett. **76**, 2511 (1996).
[9] P. M. Ajayan, O. Stephan, C. Colliex, and D. Trauth, Science **265**, 1212 (1994).
[10] P. Calvert, Nature (London) **357**, 365 (1992).
[11] T. W. Ebbesen, Annu. Rev. Mater. Sci. **24**, 235 (1994).
[12] P. M. Ajayan, Condens. Matter News **4**, 9 (1995).
[13] A. Kelly and N. H. MacMillan, *Strong Solids* (Clarendon Press, Oxford, 1986), 3rd ed., p. 6.
[14] J. Prescott, *Applied Elasticity* (Dover Publications, New York, 1946), p. 100.
[15] R. Feynman, R. Leyton, and M. Sands, *The Feynman Lectures in Physics* (Addison-Wesley, Reading, MA, 1964), Vol. 2.
[16] S. Timoshenko, *Theory of Elastic Stability* (McGraw-Hill, New York, 1936), Chaps. 2 and 9.
[17] Y. Lanir and Y. C. B. Fung, J. Compos. Mater. **6**, 387 (1972).
[18] H. Allen and P. Bulson, *Background to Buckling* (McGraw-Hill, London, 1980), Chap. 7; A. H. Cottrell, *The Mechanical Properties of Matter* (John Wiley & Sons, New York, 1964), Chap. 5.
[19] The morphological singularities under stress predicted by Yakobson *et al.* [8] were calculated for free nanotubes, and for tube structures that are intermediate between the geometries for buckling and collapse observed here. Indeed, assuming that h is equal to the length of a C-C bond (0.14 nm), with $D = 1$ nm and $L = 6$ nm [8], one has $h/r \approx 0.29$ and $(L/r)_{\text{min}} \approx 12$, which is transitional between the values of the same parameters for buckling [for which $h/r \approx 0.72$ and $(L/r)_{\text{min}} \approx 16.4$] and collapse [for which $h/r \approx 0.08$ and $(L/r)_{\text{min}} \approx 11$] observed here. The results presented here and those of Yakobson *et al.* may therefore be fully compatible.
[20] For thin-walled tubes we have used Euler's expression as an approximation, since it is strictly valid for full rods only. It may be adapted to the case of hollow rods by using $I = (p/4)(4hr^3 + 4h^3r - 6h^2r^2 - h^4)$ for the area moment of inertia, and $A = \pi(2rh - h^2)$ for the tube cross section. Using $\xi = h/r$, the resulting expression for the Euler stress is $\sigma = E(\pi r/l)^2 f(\xi)$, where the function $f(\xi) = (4\xi + 4\xi^3 - 6\xi^2 - \xi^4)/(2\xi - \xi^2)$ decreases monotonically to 1 as ξ tends to 1.